Hindawi
Journal of Food Quality
Volume 2021, Article ID 3925572, 11 pages
https://doi.org/10.1155/2021/3925572

Research Article

Hygroscopic Properties of Sweet Cherry Powder: Thermodynamic Properties and Microstructural Changes

Rachida Ouaabou,[1] **Said Ennahli**,[2] **Chira Di Lorenzo**,[3] **Hafida Hanine**,[4] **Aadil Bajoub**,[2] **Rachid Lahlali**,[2] **Ali Idlimam**,[5] **Ahmed Ait Oubahou**,[6] **and Mohamed Mesnaoui**[1]

[1]*Department of Chemistry, Faculty of Sciences Semlalia, Cadi Ayyad University, 40000 Marrakech, Morocco*
[2]*National School of Agriculture of Meknes, ENAM, Meknes, Morocco*
[3]*Department of Pharmacological and Biomolecular Sciences, University of Milan, Milan, Italy*
[4]*Faculty of Sciences and Technology, University Sultan Moulay Slimane, BP 523, Beni-Mellal, Morocco*
[5]*Department of Physics, Cadi Ayyad University, 40000 Marrakech, Morocco*
[6]*Institut Agronomique et Vétérinaire Hassan II, Agadir, Morocco*

Correspondence should be addressed to Said Ennahli; ennahlisaid@gmail.com

Received 29 April 2021; Revised 20 October 2021; Accepted 5 November 2021; Published 1 December 2021

Academic Editor: Vicente M. G mez L pez

Understanding sorption isotherms is crucial in food science for optimizing the drying processes, enhancing the shelf-life of food, and maintaining food quality during storage. This study investigated the isotherms of sweet cherry powder (SCP) using the static gravimetric method. The experimental water sorption curves of lyophilized sweet cherry powder were determined at 30°C, 40°C, and 50°C. The curves were then fitted to six isotherm models: Modified GAB, Halsey, Smith, Oswin, Caurie, and Kühn models. To define the energy associated with the sorption process, the isosteric sorption heat, differential entropy, and spreading pressure were derived from the isotherms. Among the six models, the Smith model is the most reliable in predicting the sorption of the cherry powder with a determination coefficient (R^2) of 0.9978 and a mean relative error (MRE) ≤1.61. The values of the net isosteric heat and differential entropy for the cherry increased exponentially as the moisture content decreased. The net isosteric heat values varied from 10.63 to 90.97 kJ mol^{-1}, while the differential entropy values varied from 27.94 to 273.39 J. $mol^{-1}K^{-1}$. Overall, the enthalpy-entropy compensation theory showed that enthalpy-controlled mechanisms could be used to regulate water adsorption in cherry powders.

1. Introduction

Sweet cherries (*Prunus avium* L.) are highly perishable fruits due to their high moisture content and respiration rate, which results in a rapid deterioration of the fruit within a few days. However, this fruit can be preserved through proper drying while maintaining its quality. The purpose of drying is to inhibit the proliferation of microorganisms. By limiting both the enzymatic and nonenzymatic browning reactions in the material matrix, the sensorial characteristics and the nutritional value of the food product are maintained [1]. Dried cherry powders have numerous uses in the food industry, such as additives, in the beverage industry [2]. Additionally, cherry powders can be used as high fiber fortifiers and are often incorporated as ingredients in instant noodles, dried soups, and other food recipes [3–6]. In the nutraceutical industry, cherry powders are added to various food products to help consumers build immunity [3, 7].

However, improper food storage conditions can result in a significant decrease in the quality of cherry powders over time. This explains why water sorption isotherms are useful thermodynamic tools for predicting the interaction between water and food components. Moreover, sorption isotherms can be used to explore the structural features of cherry

powders, such as specific surface area, pore volume, pore size distribution, and crystallinity [8–10]. Such data are key elements for optimizing storage conditions and packaging, and they can be used in the food industry to improve the aroma retention, color, texture, nutrients [11], and biological stability of food products [12].

Furthermore, the moisture sorption isotherms of foods provide valuable information for developing new food products and predicting the food shelf-life [13]. This scientific tool can also be utilized for preserving and storing seasonal fruits to make food available to consumers year-round [14]. In the food industry, sorption isotherms data are advantageous in monitoring drying processes, determining the optimum residual moisture content of the final product [15], and calculating the drying time of hygroscopic substances [16]. Furthermore, sorption isotherms can be used to compute the enthalpy, entropy, and free-energy values required for food preservation [17, 18]. The moisture sorption data can also provide insights into the surface area and the number of surface binding sites of materials [19].

Sorption isotherms can be determined experimentally. First, food samples are equilibrated at constant temperatures in the atmosphere with different values of relative humidity. After equilibration, the water (moisture) content of the samples is analyzed. Each pair of the equilibrium relative humidity (ERH) moisture content data provides one point on the isotherm. Nonetheless, the experimental methods for determining sorption isotherms are categorized into two groups: static and dynamic procedures [20]. The static gravimetric method usually involves the placement of the fruit samples in desiccator jars with different saturated salt solutions. The samples are then left for some time to equilibrate at a constant temperature. At a constant temperature, the concentration of the saturated solutions and their water vapor pressure is kept constant. Unlike the static methods, in the dynamic methods, the samples are equilibrated with a gas stream, and the relative humidity of the samples is changed continuously. The quantity of the moisture adsorbed or desorbed is determined by recording the change in the sample weight. However, numerous attempts have been made to develop mathematical models that can predict sorption isotherms [21]. Current prediction models are limited by metrics based on physical theories of adsorption or curve-fitting techniques.

This study was undertaken to determine the sorption isotherms for the sweet cherry powder at three temperatures (30°C, 40°C, and 50°C) using the static gravimetric method. In addition, analytical models were selected to adjust the experimental data, and the thermodynamic properties (differential enthalpy, differential entropy, Gibbs free energy, and spreading pressure) for predicting isotherms as well as the microstructural changes were investigated.

2. Materials and Methods

2.1. Raw Material. Sweet cherries (*Prunus avium* L.) of *Burlat* variety were harvested in June 2019 in the Meknes region in Morocco. The fruits were pitted and freeze-dried at −55°C under vacuum (4.5 Pa) for 96 h using a Freeze Dryer (ALPHA 1–4 LDplus/ALPHA 2–4 LDplus). The dried product was later crushed and sifted with a vibratory sieve shaker (Cisa/BA200 N) to obtain a fine powder with particle diameters between 50 and 125 μm. The fruit powder was then kept in a sealed glass flask at 4°C.

2.2. Characterization Techniques. The microstructure of the lyophilized cherry was examined with a scanning electron microscopy electron microscope (SEM) (TESCAN VEGA 3) operating at 20 kV. Samples were carbon-sputtered and photographed at different magnifications. Thermal gravimetric-differential thermal analysis (TG-DTA) was used to study the thermal properties of lyophilized cherry (DTA, Labsys Evo 1600, SETARAM). The process consists of heating ~50 mg of sample in a platinum crucible from ambient temperature to 800°C at a heating rate of 10°C min^{-1}.

2.3. Sorption Isotherms Experiments. The adsorption isotherm was determined by the static gravimetric method. The salt water activity (a_w) ranged from 0.074 to 0.898, 0.063 to 0.891, and 0.057 to 0.882 at 30°C, 40°C, and 50°C, respectively. Powder samples (2 g) were first placed inside 1 L sealed glass jars containing saturated salt solutions. The water activities values of each salt solution as a function of temperature were described by Bizot and Multon [22]. The glass jars were kept in evacuated desiccators at the corresponding temperature (±1°C) and then weighed periodically until equilibrium was reached. After reaching equilibrium (when three consecutive measures were the same), the samples are weighed (M_h) and placed in a drying oven at 105°C for 24 h to measure the dry mass (M_s). All the moisture adsorption measurements were replicated three times. The percentage difference in the equilibrium moisture contents between triplicate samples was, on average, less than 1% of the mean of the three values.

The equilibrium moisture content (EMC) of the product at hygroscopic equilibrium is obtained by applying

$$\mathrm{EMC} = X_{eq} = \frac{M_h - M_s}{M_s}. \quad (1)$$

2.4. Modeling Equations. The moisture sorption isotherms of lyophilized sweet cherries powder were analyzed using six mathematical equations: Modified GAB (Guggenheim–Anderson–Boer), Halsey, Smith, Oswin, Caurie, and Kühn models (Table 1). The equations were selected to fit the experimental sorption. All calculations were performed using Curve Expert Professional 2.3.

The Curve Expert Professional 2.3. was used to determine the model parameters and calculate the 95% confidence intervals of the parameters. Apart from the adjusted determination coefficient (R^2 adj), the goodness of the fitting model was tested using the root mean square error (RMSE), and the mean relative percentage deviation (P%) was used to determine the quality of the fit between predicted and experimental values.

Table 1: Moisture sorption isotherm models used to analyze data for SCP.

Models	Mathematical expression	References
Modified GAB	$X_{eq} = A.B.(C/T).(a_w/(1 - B.a_w).(1 - B.a_w + B.(C/T).a_w))$	[54]
Halsey	$X_{eq} = b_1.b_2.(a_w/(1 - a_w)(1 - a_w + b_2.a_w))$	[55]
Smith	$X_{eq} = b_1 - b_2.\ln(1 - a_w)$	[56]
Oswin	$X_{eq} = b_1.(a_w/(1 - a_w))^{b_2}$	[57]
Caurie	$X_{eq} = e^{(b_1+b_2.a_w)}$	[58]
Kühn	$X_{eq} = (b_1/\ln a_w) + b_2$	[59]

These parameters were calculated using equations (2)–(4), respectively.

$$R = \frac{\sum_{i=1}^{N}\left(X_{eq_{i,pre\,d}} - \overline{X}_{eq_{i,\exp}}\right)^2}{\sum_{i=1}^{N}\left(X_{eq_{i,\exp}} - \overline{X}_{eq_{i,\exp}}\right)^2}, \quad (2)$$

$$P = \frac{100}{N} \times \sum_{i=1}^{N}\left|\frac{X_{eq_{i,\exp}} - X_{eq_{i,pre\,d}}}{X_{eq_{i,\exp}}}\right|, \quad (3)$$

$$\mathrm{RMSE} = \sqrt{\sum_{i=1}^{n}\frac{\left(X_{eq_{i,pre\,d}} - X_{eq_{i,\exp}}\right)^2}{N}}, \quad (4)$$

where $X_{eq_{i,\exp}}$ is the experimental moisture content (% d.b.), $X_{eq_{i,pre\,d}}$ is the predicted moisture content (% d.b.), N is the number of data points, and d.b. is the dry weight basis.

It is generally assumed that a good fit is obtained with high values of R^2 adj ≥0.9 and low values of RMSE and P (lower than 10% d.b.).

2.5. Thermodynamic Properties. The differential enthalpy, commonly referred to as the net isosteric heat of sorption q_{st}, describes the state of the absorbed water by the solid material. At a constant moisture content, the net isosteric heat, q_{st} (kJ mol^{-1}), was calculated using the equation derived from the Clausius–Clapeyron equation:

$$q_{st} = -R\left[\frac{d(\ln a_w)}{d(1/\theta)}\right]X_{eq}, \quad (5)$$

where a_w is the water activity (dimensionless), θ is the absolute temperature (K), and R is the universal gas constant (J/(mol K)).

By assuming that q_{st}, is invariable with the temperature for a given EMC, the integration of equation (5) gives [23]

$$\ln a_w = \frac{-q_{st}}{R}\frac{1}{T} + \frac{\Delta S}{R}, \quad (6)$$

where ΔS is the differential entropy of sorption (J/kmol).

The plot of $\ln(a_w)$ versus $1/T$ gives a straight line with a slope of q_{st}/R and an intercept of $\Delta S/R$, which are used to estimate the isosteric sorption heat q_{st} and the differential entropy ΔS, respectively.

The Gibbs free energy is calculated using the following equation [24]:

$$\Delta G = RT\ln(a_w). \quad (7)$$

According to the compensation theory [25], the linear relation between enthalpy and entropy for a specific reaction is computed with the following equation:

$$q_{st} = T_\beta \Delta S + \Delta G_\beta. \quad (8)$$

The isokinetic temperature (T_β) represents the temperature at which all reactions in the series proceed at the same rate. The Gibbs free-energy (ΔG_β) values at T_β can be used to indicate the spontaneity of the sorption process. More specifically, the Gibbs free energy is considered spontaneous if the value of ΔG_β was negative and nonspontaneous if the value of ΔG_β was positive. The validation of the compensation theory is tested by comparing the isokinetic temperature with the harmonic mean temperature (T_{hm}). Mathematically, T_{hm} is represented as follows:

$$T_{hm} = \frac{n}{\sum_1^n (1/T)}. \quad (9)$$

The enthalpy-entropy compensation theory can be applied only if $T_\beta \neq T_{hm}$. The thermodynamic properties are evaluated at a constant spreading pressure, which equals the force applied on the plane of the surface to prevent the surface from diffusion [26]. This parameter is the surface energy and is defined as the increase in surface tension of bare sorption sites due to absorbed or adsorbed molecules [27]. This key parameter is dependent on both moisture content and water activity and calculated as

$$\pi = \frac{K_B T}{A_m}\int_0^{a_w}\frac{\theta}{a_w}\mathrm{d}a_w, \quad (10)$$

where k_B is Boltzmann constant (1.380×10^{-23} JK^{-1}), A_m is the area of a water molecule (1.06×10^{-19} m^2), and the moisture ratio θ is given by $\theta = X_{eq}/X_m$, T (K) temperature.

The spreading pressure is defined as the force applied in the surface plane perpendicular to each unit length of the edge to retain the surface from spreading. It is calculated using the GAB model equation and defined as

$$\pi = \frac{K_B T}{A_m}\ln\left[\frac{1 - B_{a_w} + C_{a_w}}{1 - B_{a_w}}\right], \quad (11)$$

where B and C are the constants of the GAB model.

The determination of the integral thermodynamic properties (enthalpy and entropy) and the water activity–temperature conditions where the freeze-dried mucilage minimum integral entropy occurred, considered as the point of maximum storage stability, was established as indicated

by Pérez-Alonso et al. [28]. These authors have provided a thorough description of the followed procedure and equations used for this purpose.

The integral enthalpy was calculated using the Clausius–Clapeyron equation at a constant pressure of diffusion or surface potential (π) [29, 30].

$$\left(\frac{\partial \ln a_w}{\partial (1/T)}\right)_{\pi} = \frac{H_s - H_l}{R} = \frac{(\Delta H_{\text{int}})_T}{R}, \quad (12)$$

where H_s is the integral molar enthalpy of water adsorbed of the mucilage (kJ mol^{-1}), H_l is the partial molar enthalpy of adsorbed water at constant temperature and pressure (kJ mol^{-1}), R is the universal gas constant (8.314×10^{-3} kJ mol^{-1} K^{-1}), and $(\Delta H_{\text{int}})_T$ is the integral enthalpy at a constant temperature (kJ mol^{-1}). A plot in the form $\ln a_w$ vs. $1/T$, for a specific constant pressure of diffusion $(\Delta H_{\text{int}})_T$, is determined from the slope $(\Delta H_{\text{int}})_T/R$.

The integral enthalpy was needed to determine the integral entropy associated with the sorption process. It was calculated using the following equation:

$$(\Delta S_{\text{int}})_T = S_s - S_l = \frac{(\Delta H_{\text{int}})_T}{T} - R \ln a_w, \quad (13)$$

where $S_s = S/N_1$ is the integral entropy of water adsorbed in the mucilage, S_l is the partial molar entropy of adsorbed water at constant temperature and pressure (kJ mol^{-1}), and $(\Delta S_{\text{int}})_T$ is the integral entropy at a constant temperature.

Using equation (14), the water surface area (S_0), is defined as follows:

$$S_0 = M_m \times \frac{1}{PM_{\text{H}_2\text{O}}} \times N_0 \times A_{\text{H}_2\text{O}} = 3.5 \times 10^3 \times M_m, \quad (14)$$

where M_m is the monolayer moisture content, N_0 is the Avogadro constant (6×10^{23} molecules per mole), and $PM_{\text{H}_2\text{O}}$ and $A_{\text{H}_2\text{O}}$ are the molecular weight of water (18 g mol^{-1}) and the area of the water molecule (10.6×10^{-20} m^2), respectively.

3. Results and Discussion

3.1. Scanning Electron Microscopy Analysis. The effect of the freeze-drying process on the powder microstructure was observed under a scanning electron microscope (Figure 1). All powder samples looked similar. When freeze-dried, the particles were not spherical and agglomerated together; they adhered under the freeze-drying and ice development often bonded the cells together, therefore making the distinction between separate cells difficult. The grinding of freeze-dried cherries into powder form resulted in more irregularly shaped particles; similar results were reported by Caparino et al. on freeze-dried mango powder [31]. Freeze-dried powders exhibited high porosity and stretched pore shape, while porous structures are easy to rehydrate than compact ones, and the freeze-dried powder structure could include closed pores, which can be an obstacle for mass transfer during rehydration [32]. The freeze-drying process of TPC at −55°C may have impacted the microstructure. Lin [33] demonstrated that freeze-drying algal powders between −30°C and −60°C resulted in the formation of large ice crystals that grow in the intercellular spaces causing mechanical damage to the cells. Such mechanical damage was reduced significantly when the cells were rapidly frozen at −196°C. Similar observations were reported by Voda et al. [34], who found that freeze-drying carrots at a very low temperature (−196°C) had a significant impact on the microstructure of carrot as compared to a lower temperature (−28°C).

3.2. Thermal Behavior. The thermal curve generated from the differential thermal analysis data is represented in Figure 2. Three distinct regions of weight loss (120–215°C; 215–323°C; 323–800°C) are observed. The first region (120°C to 215°C) showed a mass loss of 5%, mainly due to the removal of the physically adsorbed water and other volatile substances [35]. The second region (215°C to 323°C) recorded a significant drop in mass (34.92%). This observation is likely attributed to more profound and complex volatilization of matter such as decarboxylation of the powder rich-polysaccharides like pectin [35, 36]. The third region (323°C–800°C) accounts for 52.23% of mass drop and is likely the residue left after incineration (82.92%) at 800°C. Similar trends were reported in tropical fruit powders [36, 37]. The TGA allowed us to identify the mass losses as a function of temperature, and the DTA analysis confirmed the results of the TGA by assigning each loss a peak (exothermic or endothermic) which validates the losses obtained. TGA and DTA also showed mass losses with an increase in temperature and heating rate [38].

3.3. Sorption Isotherms. The experimental data of the equilibrium water content versus water activity of tested salt solutions at different temperatures are shown in Table 2 and Figure 3. The increase in temperature resulted in a decrease in the X_{eq} of the powder samples. As the temperature increased, the water molecules became excited, thereby weakening the attraction forces between them and decreasing the equilibrium moisture content [39]. Figure 3 shows the experiment values and the estimates obtained with the Smith model at 30°C, 40°C, and 50°C. It displays the isotherms represented by the sigmoidal form and corresponds to Type II isotherms according to the classification of IUPAC (International Union of Pure and Applied Chemistry). Type II isotherms are typical for food products with high sugar content, such as polysaccharides and proteins [40]. The hygroscopic equilibrium of sweet cherry powder was reached in 10 days.

3.4. Optimal Storage Conditions. The moisture sorption isotherm defines the relationship between the equilibrium of the moisture content and the water activity at a constant temperature of a given food product. It is a critical factor in designing and optimizing drying equipment, designing food packages, forecasting moisture changes during storage, and predicting food quality, stability, and shelf-life [41]. Here, we determined the optimum equilibrium relative humidity for

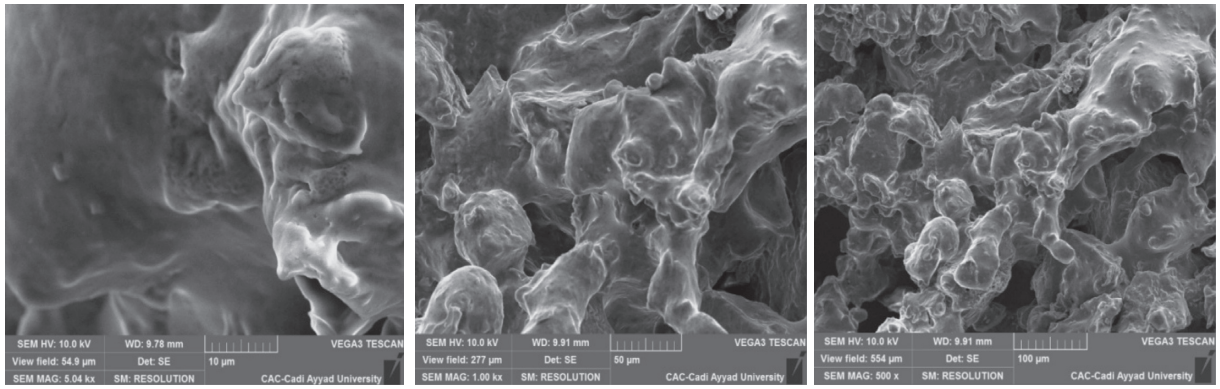

Figure 1: Scanning electron microscopy (SEM) images of SCP.

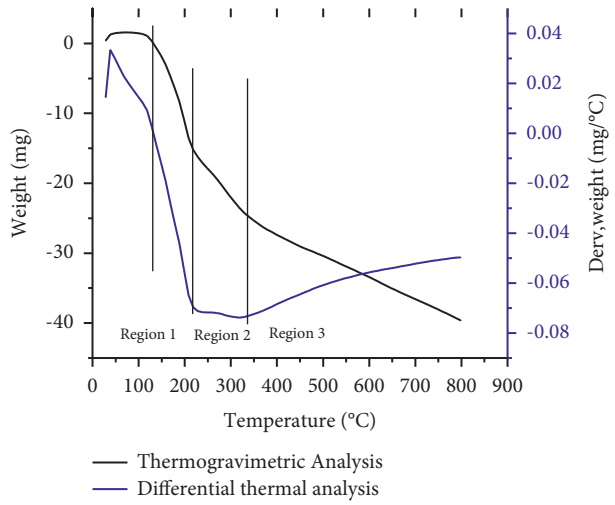

Figure 2: Thermogravimetry analysis.

Table 2: Equilibrium water content Xeq (d.b.).

Temperature (°C)	KOH	($MgCl_2$, $6H_2O$)	K_2CO_3	$NaNO_3$	KCl	($BaCl_2$, $2H_2O$)
30	0.1875 ± 0.0093	0.2751 ± 0.0137	0.3245 ± 0.0162	0.4569 ± 0.0228	0.5745 ± 0.0287	0.6964 ± 0.0348
40	0.1476 ± 0.0074	0.2364 ± 0.0118	0.2724 ± 0.0136	0.3902 ± 0.0195	0.4846 ± 0.0242	0.6345 ± 0.0317
50	0.1113 ± 0.0055	0.1913 ± 0.0095	0.2286 ± 0.0114	0.3556 ± 0.0177	0.4452 ± 0.0222	0.5762 ± 0.0288

the storage of cherry powder. The sorption isotherm can be modeled under a 3rd-degree function, and the central part or "plate" corresponds to the zone of better stability of the products. This calculation process consists of making a polynomial decomposition of the equilibrium water content. By doing this, it is possible to calculate the value for which the derivative second is canceled (no inflection) and subsequently determine the optimal relative humidity of the conservation.

The value of the optimal water activity for SCP conservation was 0.39 (Figure 4). This result aligns with the optimal water activities reported in the literature (0.2–0.4) [16, 42]. A polynomial equation of the equilibrium moisture content based on the water activity of SCP is as follows:

$$X_{eq} = 310.58a_w^3 - 393.31a_w^2 + 175.73a_w. \quad (15)$$

To reinforce this method, the integral entropy that provides information on the maximum stability of water molecules in the food matrix was calculated. Figure 5 shows the integral entropy as a function of moisture content at 30°C, 40°C, and 50°C. The integral entropy of adsorption increased with the increase in the equilibrium moisture content. This increase translates to the increase in the degrees of freedom of the water in the product, which increased with the equilibrium moisture content; therefore, a less structured system is described. The minimum integral entropy is considered as that of maximum stability because it is where water molecules achieve a more ordered

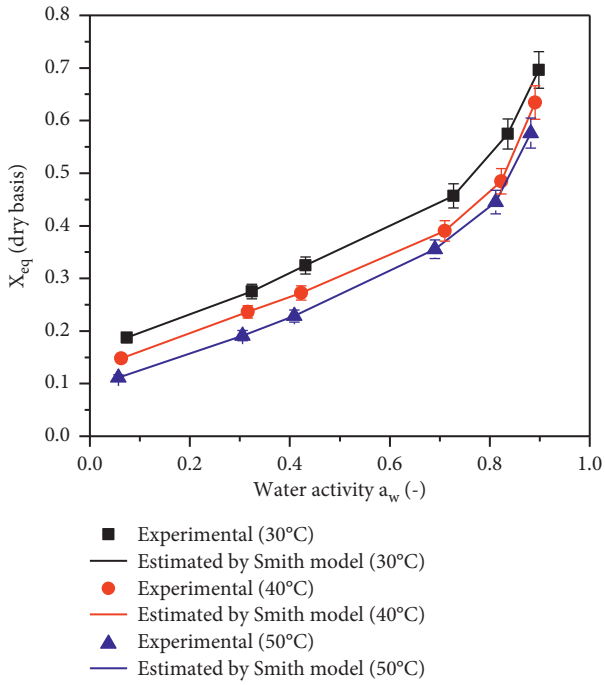

Figure 3: Adsorption isotherms of SCP at different temperatures.

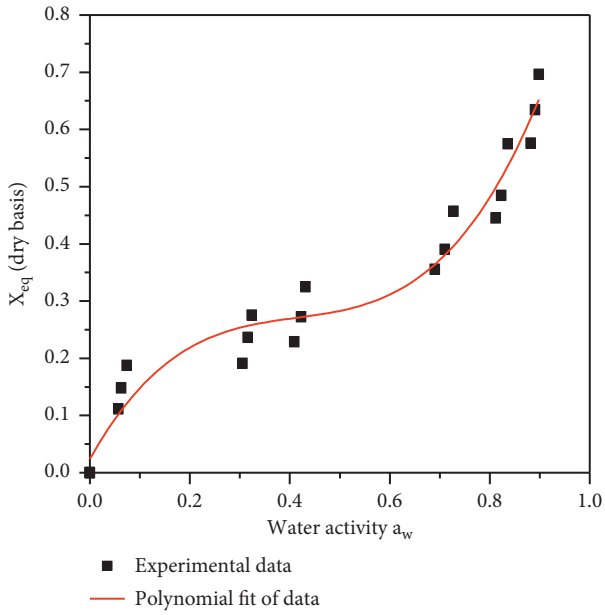

Figure 4: Optimal water activity for SCP conservation.

arrangement within the solid and strong bonds between the adsorbate and the adsorbent; thus, water is less available to participate in spoilage reactions [43]. Thus, with the results seen in Figure 5, the optimal water activity for maximum stability of SCP was 0.39.

3.5. Modeling of the Sorption Isotherms. To describe the moisture sorption isotherms, the data sorption curves of the cherry powder were fitted to six models. The adjustment results for the sorption models considering the effect of temperature on the isotherms of adsorption were represented in Table 3, including the adjusted determination coefficient R^2_{adj}, root mean square error (RMSE), and percent average relative deviation (P). Statistical processing indicates the acceptability of considered models for the prediction of the equilibrium moisture content of the sweet cherry powder. The best fit was attributed to the model which possesses a higher value of "R^2_{adj}" and lower values of RMSE and P [44].

The sorption isotherm analysis showed that the Smith model fits the equilibrium data well because it has the highest R^2_{adj} (0.997) and the lowest RMSE (0.017) and P (1.7003%) values. In addition, the confidence intervals showed that all parameters of the model were statistically significant at a confidence level of 95%, indicating a good fit for practical purposes [45]. This model was found to be suitable with different foods: pistachio [46], banana flour [47], and extruded snacks [48]. The analysis of the residuals values versus the predicted EMC values of sorption is in agreement with the previous results.

The monolayer moisture content (Xo) measures the number of sorption sites and is regarded as the optimum value for food stability [49]. Below this value, the rates of deteriorative reactions are at their minimal values [50]. It was found that the monolayer moisture content obtained from the GAB model (Table 3) decreased as the temperature increased. This was attributed to the weakening of hydrogen bonds as the temperature of the water molecules increased. The estimated values for Xo were within the range of values for agrofood products [49]. Furthermore, the K constant increased as the temperature increased. The physical measuring of K is related to the adsorption heat of the multilayer. Similar findings were reported by Aksil et al. [51], who used the GAB model to explore the sorption isotherm of lyophilized *Arbutus unedo* L. powder. The parameter C was not dependent on temperature dependence, and it was within the range of 5.67 and ∞, as indicated by Ruiz-López and Herman-Lara [44].

3.6. Thermodynamic Properties

3.6.1. Sorption Heat and Differential Entropy. The evolution of the net isosteric heat and differential entropy as a function of water content is shown in Figure 6(a). The net isosteric sorption heat was significantly dependent on the moisture content. More specifically, the net isosteric sorption heat decreased rapidly from 90.97 to 10.03 kJ mol^{-1} as the equilibrium moisture content increased. The observed increase in the net isosteric heat at low moisture content could be traced to the abundance of active binding sites on the surface of the materials. Once the binding sites were covered with monolayer water molecules, they became less active and thus generated lower heat of sorption [52]. At low moisture content, q_{st} decreased gradually while approaching zero. This means that the isosteric heat was equal to the water condensation heat. The corresponding moisture content could be considered as the limit of "bound" water [24].

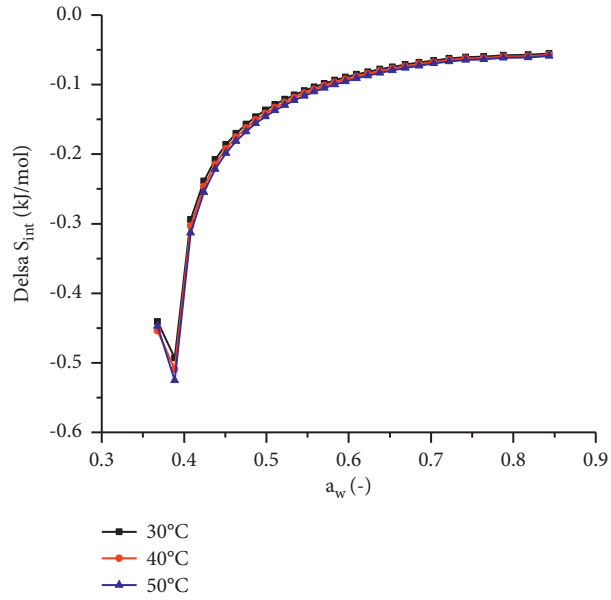

Figure 5: Integral entropy of SCP at temperatures of 30°C, 40°C, and 50°C.

Table 3: Estimated parameters of models for SCP at different temperatures of adsorption curves.

Models	Parameters	Confidence intervals 95%	R^2_{adj}	RMSE	P (%)
Modified GAB	$A = 0.2003\%$ d,b	[0.0018, −0.3818]	0.9912	0.0419	9.6201
	$B = 0.8287$	[0.5571, −1.022]			
	$C = 0.9806\ K^{-1}$	[−0.3075, −2.2573]			
Halsey	$b_1 = 0.0822\ K^{-1}$	[0.069, 0.0954]	0.9128	0.1129	6.1873
	$b_2 = 1.126\ K^{-1}$	[−1.655, 1.655]			
	$b_{1.2} = 9.3113$	[0.0501, −0.1119]			
Smith	$b_1 = 0.1418\ K^{-1}$	[0.103, 0.1828]	0.9988	0.039	1.3209
	$b_2 = 0.2176\ K^{-1}$	[0.1805, 0.2426]			
	$b_{2.1} = 1.067$	[0.0818, 0.1317]			
Oswin	$b_1 = 0.3062\ K^{-1}$	[0.3293, 0.3768]	0.9763	0.039	1.7015
	$b_2 = 0.3376\ K^{-1}$	[0.263, 0.3428]			
	$b_{2.1} = 0.3415$	[0.2717, 0.3347]	0.9875	0.0222	2.2262
Caurie	$b_1 = -2.071\ K^{-1}$	[−2.1613, −1.521]	0.9889	0.0328	3.2818
	$b_2 = 1.7483$	[1.1709, 1.9909]			
	$b_{2.2} = 2.538$	[0.9819, 0.0378]			
Kühn	$b_1 = -5.399\ K^{-1}$	[−5.709, 5.692]	0.9653	0.0132	5.2741
	$b_2 = 2.348\ K^{-1}$	[−1.363, 1.3593]			
	$b_{1.2} = -5.458$	[−0.2184, 0.2184]			

The differential entropy of isotherms (ΔS) was calculated using equation (6). The determination of the differential entropy variation provides information about the thermal energy losses ($T\ \Delta S$) in the system and the irreversibility of this physical phenomena, especially during thermal exchanges. Differential sorption enthalpies of the sampled cherry powder at temperatures ranging between 30°C and 50°C are indicated in Figure 6(b). As for q_{st}, the differential entropy decreased from 273.39 to 27.94 $J\,mol^{-1}\,K^{-1}$ with the increase in the equilibrium moisture content. This shows that high water molecules coverage reduced the mobility of the latter.

3.6.2. Enthalpy-Entropy Compensation. The compensation theory for cherry powder is illustrated in Figure 7. According to this theory, for a specific reaction, enthalpy has a linear relationship with entropy. The Gibbs free energy (ΔG) and isokinetic temperature were calculated using equation (8). The enthalpy-entropy relationship for the cherry powder is mathematically represented as follows:

$$q_{st} = 328.59\Delta S + 1176.58. \quad (16)$$

The free-energy value for cherry powder was positive, meaning that the isotherms of the powder are an endergonic nonspontaneous reaction, which requires an input of energy from the surrounding environment of the product.

With regard to the compensation enthalpy-entropy theory, the isokinetic temperature (T_β) and the harmonic temperature (T_{hm}) are significantly different from each other. The calculated harmonic temperature (T_{hm}) was 312.94 K while the observed isokinetic temperature value

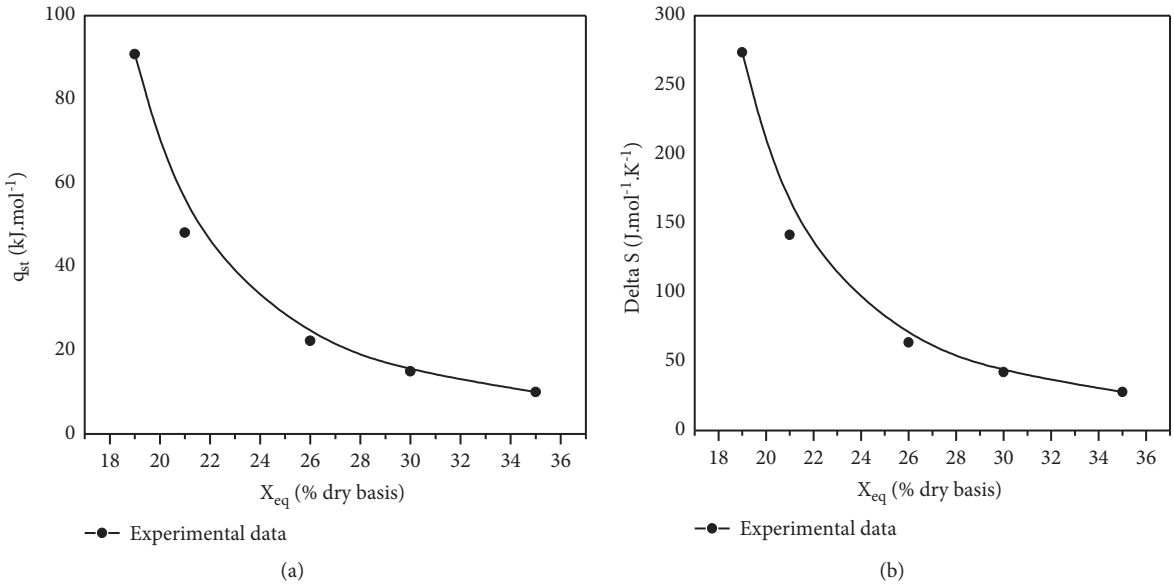

Figure 6: Relationships between equilibrium moisture content and (a) isosteric heat and (b) differential entropy.

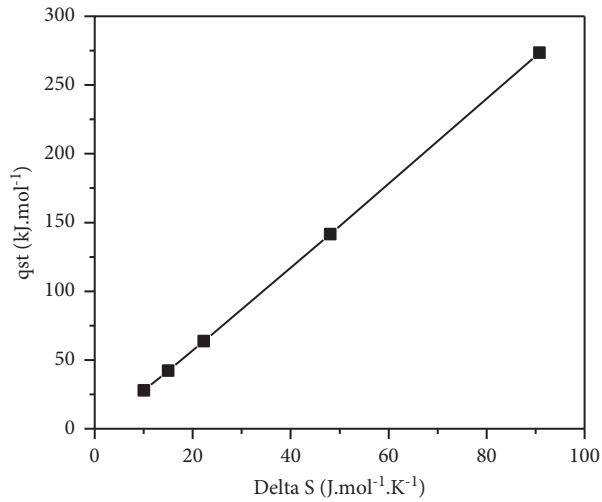

Figure 7: Enthalpy-entropy compensation theory for the water adsorption processes in SCP.

was close to the T_{hm} value. This difference supports the enthalpy-entropy compensation theory. Our data showed that (T_β) is higher than (T_{hm}). Therefore, the adsorption process is enthalpy-driven. This reveals that the microstructure of the powder is quite stable and did not face any changes during water adsorption within the temperature range of 30 to 50°C.

3.6.3. Spreading Pressure. The spreading pressure of the powder samples at different temperatures was determined using equations (10) and (11) and shown in Figure 8. The spreading pressure values increased as the water activity increased. The sinusoidal behavior of the isotherm was expected to disappear at a given temperature. Therefore, spreading pressure might have a linear dependence versus a_w. The observed high spreading pressure values at a lower temperature indicated a high affinity of water molecules to active sites, in part because of the structure and the chemical composition of the cherry. In their research, Al-Muhtaseb et al. [53] found the same behavior in starch powders.

3.6.4. Surface Area. Specific surface provides insight into the water-binding properties of a given material and is calculated using equation (14). The monolayer moisture values generated by the GAB model were 63.21, 52.08, and 44.98 ($m^2\,g^{-1}$ dry solids) for the corresponding equilibrium temperatures of 30°C, 40°C, and 50°C, respectively. A decrease in moisture was observed as the temperature increased. This relationship has been linked to a decrease in the number of active sites as a response to chemical and physical changes driven by higher temperatures.

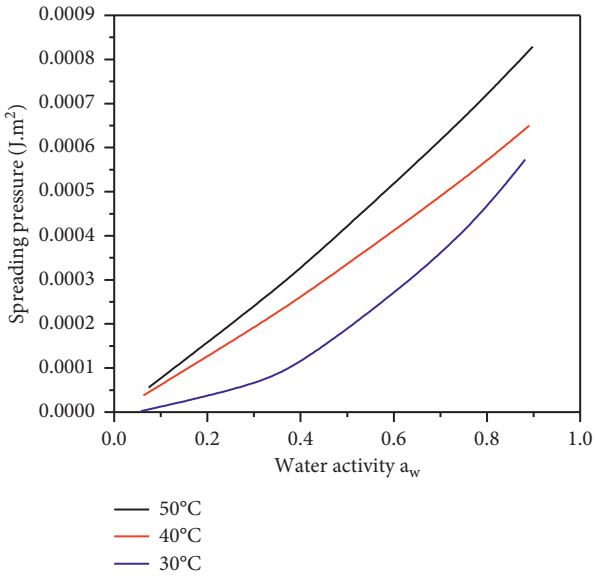

Figure 8: Spreading pressure isotherms at different temperatures.

4. Conclusion

This study suggested that the sweet cherry powder preservation strategy is optimized by monitoring its moisture content. Findings revealed that the moisture sorption isotherms exhibited a Type II shape. An inverse relationship between temperature and equilibrium moisture content of the fruit powder was observed. Moreover, our results indicated that the experimental data fitted the Smith model best compared to GAB, Halsey, Oswin, Caurie, and Kühn models. The net isosteric sorption heat and the differential entropy were found to decrease as the equilibrium moisture content increased. Overall, the enthalpy-entropy compensation or the isokinetic theory indicated that enthalpy-controlled mechanisms could be used to regulate water adsorption in fruit powder and in turn optimizing storage condition and packaging, and they can be used in the food industry to improve aroma retention, color, nutrients, and biological stability of the food products. The SCP properties indicate the different bioactive compounds can be microencapsulated using spray drying, which will protect them against deleterious environmental factors and extend their shelf-life, when stored under proper conditions (the optimal temperature and water activity determined in this study).

Data Availability

The data that support the findings of this study are available from the corresponding author upon reasonable request and upon the approval of the MCRDV agency (Projet_Cerisier_2016).

Conflicts of Interest

The authors declare that they have no conflicts of interest.

References

[1] J. M. Aguilera, A. Chiralt, and P. Fito, "Food dehydration and product structure," *Trends in Food Science & Technology*, vol. 14, no. 10, pp. 432–437, 2003.

[2] M. E. Camire, M. P. Dougherty, and J. L. Briggs, "Functionality of fruit powders in extruded corn breakfast cereals," *Food Chemistry*, vol. 101, no. 2, pp. 765–770, 2007.

[3] J. M. C. D. Costa, É. M. D. F. Felipe, G. A. Maia, F. F. F. Hernandez, and I. M. Brasil, "Production and characterization of the cashew apple (anacardium occidentalel.) and guava (Psidium guajaval.) fruit powders," *Journal of Food Processing and Preservation*, vol. 33, pp. 299–312, 2009.

[4] C. I. Nindo, T. Sun, S. W. Wang, J. Tang, and J. R. Powers, "Evaluation of drying technologies for retention of physical quality and antioxidants in asparagus (Asparagus officinalis, L.)," *Lebensmittel-Wissenschaft und -Technologie- Food Science and Technology*, vol. 36, no. 5, pp. 507–516, 2003.

[5] D. Argyropoulos, A. Heindl, and J. Müller, "Assessment of convection, hot-air combined with microwave-vacuum and freeze-drying methods for mushrooms with regard to product quality," *International Journal of Food Science and Technology*, vol. 46, no. 2, pp. 333–342, 2011.

[6] Z. Zhang, H. Song, Z. Peng, Q. Luo, J. Ming, and G. Zhao, "Characterization of stipe and cap powders of mushroom (Lentinus edodes) prepared by different grinding methods," *Journal of Food Engineering*, vol. 109, no. 3, pp. 406–413, 2012.

[7] E. W. C. Chan, Y. Y. Lim, S. K. Wong et al., "Effects of different drying methods on the antioxidant properties of leaves and tea of ginger species," *Food Chemistry*, vol. 113, no. 1, pp. 166–172, 2009.

[8] J. A. Fernández-López, M. D. Miñarro, J. M. Angosto, J. Fernández-Lledó, and J. M. Obón, "Adsorptive and surface characterization of mediterranean agrifood processing wastes: prospection for pesticide removal," *Agronomy*, vol. 11, 2021.

[9] M. Caurie, "The unimolecular character of the classical Brunauer, Emmett and Teller adsorption equation and moisture adsorption," *International Journal of Food Science and Technology*, vol. 40, no. 3, pp. 283–293, 2005.

[10] S. Lowell, J. Shields, M. Thomas, and M. Thommes, "Characterization of porous solids and powders: surface area, pore size, and density," *Choice Reviews Online*, vol. 42, p. 5288, 2005.

[11] C. I. Beristain, E. Azuara, and E. J. Vernon-Carter, "Effect of water activity on the stability to oxidation of spray-dried encapsulated orange peel oil using mesquite gum (Prosopis juliflora) as wall material," *Journal of Food Science*, vol. 67, no. 1, pp. 206–211, 2002.

[12] S. Sablani, R. Syamaladvi, and B. Swanson, "A review of methods, data, and application of state diagrams of food systems," *Food Engineering Reviews*, vol. 2, pp. 168–203, 2010.

[13] A. H. Al-Muhtaseb, W. A. M. McMinn, and T. R. A. Magee, "Moisture sorption isotherm characteristics of food products: a review," *Food and Bioproducts Processing*, vol. 80, no. 2, pp. 118–128, 2002.

[14] A. Lebert, P. Tharrault, T. Rocha, and C. Marty-Audouin, "The drying kinetics of mint (Mentha spicata Huds.)," *Journal of Food Engineering*, vol. 17, no. 1, pp. 15–28, 1992.

[15] M. Kouhila, A. Belghit, M. Daguenet, and B. C. Boutaleb, "Experimental determination of the sorption isotherms of mint (Mentha viridis), sage (Salvia officinalis) and verbena (Lippia citriodora)," *Journal of Food Engineering*, vol. 47, no. 4, pp. 281–287, 2001.

[16] N. Wang and J. G. Brennan, "Moisture sorption isotherm characteristics of potatoes at four temperatures," *Journal of Food Engineering*, vol. 14, no. 4, pp. 269–287, 1991.

[17] O. Bensebia and K. Allia, "Analysis of adsorption-desorption moisture isotherms of rosemary leaves," *Journal of Applied Research on Medicinal and Aromatic Plants*, vol. 3, no. 3, pp. 79–86, 2016.

[18] L. Červenka, L. Hloušková, and S. Žabčíková, "Moisture adsorption isotherms and thermodynamic properties of green and roasted Yerba mate (Ilex paraguariensis)," *Food Biosci*, vol. 12, pp. 122–127, 2015.

[19] E. Alpizar-Reyes, H. Carrillo-Navas, R. Romero-Romero, V. Varela-Guerrero, J. Alvarez-Ramírez, and C. Pérez-Alonso, "Thermodynamic sorption properties and glass transition temperature of tamarind seed mucilage (Tamarindus indica L.)," *Food and Bioproducts Processing*, vol. 101, pp. 166–176, 2017.

[20] G. A. Collazos-Escobar, N. Gutiérrez-Guzman, and H. A. Vaquiro Herrera, "Modeling dynamic adsorption isotherms and thermodynamic properties of specialty ground roasted-coffee (Coffee arabica L.)," *Coffee Science*, vol. 14, no. 1, pp. 93–103, 2019.

[21] R. Boquet, J. Chirife, and H. A. Iglesias, "Equations for fitting water sorption isotherms of foods," *International Journal of Food Science and Technology*, vol. 13, no. 4, pp. 319–327, 2007.

[22] H. Bizot and J. L. Multon, "Method of reference for the measurement of the activity of water in the food substances," *Annales de Technologie Agricole*, vol. 27, pp. 441–449, 1978.

[23] Y. Teng, R. Z. Wang, and J. Y. Wu, "Study of the fundamentals of adsorption systems," *Applied Thermal Engineering*, vol. 17, no. 4, pp. 327–338, 1997.

[24] E. Tsami, "Net isosteric heat of sorption in dried fruits," *Journal of Food Engineering*, vol. 14, no. 4, pp. 327–335, 1991.

[25] J. E. Leffler, "The enthalpy-entropy relationship and its implications for organic chemistry," *Journal of Organic Chemistry*, vol. 20, no. 9, pp. 1202–1231, 1955.

[26] C. Skaar and M. Babiak, "A model for bound-water transport in wood," *Wood Science and Technology*, vol. 16, no. 2, pp. 123–138, 1982.

[27] O. O. Fasina, O. O. Ajibola, and R. T. Tyler, "Thermodynamics of moisture sorption in winged bean seed and gari," *Journal of Food Process Engineering*, vol. 22, no. 6, pp. 405–418, 1999.

[28] C. Pérez-Alonso, C. I. Beristain, C. Lobato-Calleros, M. E. Rodríguez-Huezo, and E. J. Vernon-Carter, "Thermodynamic analysis of the sorption isotherms of pure and blended carbohydrate polymers," *Journal of Food Engineering*, vol. 77, pp. 753–760, 2006.

[29] R. V. Nunes and E. Rotstein, "Thermodynamics of the water-foodstuff equilibrium," *Drying Technology*, vol. 9, no. 1, pp. 113–137, 1991.

[30] T. L. Hill, P. H. Emmett, and L. G. Joyner, "Calculation of thermodynamic functions of adsorbed molecules from adsorption isotherm measurements: nitrogen on Graphon1,2," *Journal of the American Chemical Society*, vol. 73, no. 11, pp. 5102–5107, 1951.

[31] O. A. Caparino, J. Tang, C. I. Nindo, S. S. Sablani, J. R. Powers, and J. K. Fellman, "Effect of drying methods on the physical properties and microstructures of mango (Philippine 'Carabao' var.) powder," *Journal of Food Engineering*, vol. 111, no. 1, pp. 135–148, 2012.

[32] C. Perera and M. Shafiur Rahman, "Drying and food preservation," in *Handbook of Food Preservation*, pp. 173–216, Routledge, London, UK, 2007.

[33] L. P. Lin, "Microstructure of spray-dried and freeze-dried microalgal powders," *Food Microstructure*, vol. 4, pp. 341–348, 1985.

[34] A. Voda, N. Homan, M. Witek et al., "The impact of freeze-drying on microstructure and rehydration properties of carrot," *Food Research International*, vol. 49, no. 2, pp. 687–693, 2012.

[35] C. G. Mothé and M. A. Rao, "Thermal behavior of gum Arabic in comparison with cashew gum," *Thermochimica Acta*, vol. 357-358, pp. 9–13, 2000.

[36] L. M. Pereira, S. M. Carmello-Guerreiro, and M. D. Hubinger, "Microscopic features, mechanical and thermal properties of osmotically dehydrated guavas," *Lebensmittel-Wissenschaft und -Technologie- Food Science and Technology*, vol. 42, no. 1, pp. 378–384, 2009.

[37] K. A. Athmaselvi, C. Kumar, M. Balasubramanian, and I. Roy, "Thermal, structural, and physical properties of freeze dried tropical fruit powder," *Journal of Food Processing*, vol. 2014, Article ID 524705, 10 pages, 2014.

[38] Y. El may, M. Jeguirim, S. Dorge, G. Trouvé, and R. Said, "Study on the thermal behavior of different date palm residues: characterization and devolatilization kinetics under inert and oxidative atmospheres," *Energy*, vol. 44, no. 1, pp. 702–709, 2012.

[39] J. V. García-Pérez, J. A. Cárcel, G. Clemente, and A. Mulet, "Water sorption isotherms for lemon peel at different temperatures and isosteric heats," *Lebensmittel-Wissenschaft und -Technologie- Food Science and Technology*, vol. 41, pp. 18–25, 2008.

[40] H. R. Gazor and H. Chaji, "Equilibrium moisture content and heat of desorption of saffron," *International Journal of Food Science and Technology*, vol. 45, no. 8, pp. 1703–1709, 2010.

[41] H. Machhour, A. Idlimam, M. Mahrouz, I. El Hadrami, and M. Kouhila, "Sorption isotherms and thermodynamic properties of peppermint tea (Mentha piperita) after thermal and biochemical treatment," *Journal of Materials and Environmental Science*, vol. 3, pp. 232–247, 2012.

[42] H. Moussaoui, Y. Bahammou, A. Idlimam, A. Lamharrar, and N. Abdenouri, "Investigation of hygroscopic equilibrium and modeling sorption isotherms of the argan products: a comparative study of leaves, pulps, and fruits," *Food and Bioproducts Processing*, vol. 114, pp. 12–22, 2019.

[43] R. Moreira, F. Chenlo, J. Sineiro, S. Arufe, and S. Sexto, "Water sorption isotherms and air drying kinetics of fucus vesiculosus Brown seaweed," *Journal of Food Processing and Preservation*, vol. 41, 2017.

[44] I. I. Ruiz-López and E. Herman-Lara, "Statistical indices for the selection of food sorption isotherm models," *Drying Technology*, vol. 27, pp. 726–738, 2009.

[45] G. Andres Collazos-Escobar, N. Gutierrez Guzman, H. Alexander Vaquiro Herrera, and C. Milena Amorocho Cruz, "Moisture dynamic sorption isotherms and thermodynamic properties of parchment specialty coffee (Coffea arabica L.)," *Coffee Science*, vol. 15, pp. 1–10, 2020.

[46] M. Yazdani, P. Sazandehchi, M. Azizi, and P. Ghobadi, "Moisture sorption isotherms and isosteric heat for pistachio," *European Food Research and Technology*, vol. 223, no. 5, pp. 577–584, 2006.

[47] J. M. Cardoso and R. d. S. Pena, "Hygroscopic behavior of banana (Musa ssp. AAA) flour in different ripening stages," *Food and Bioproducts Processing*, vol. 92, no. 1, pp. 73–79, 2014.

[48] S. A. Wani and P. Kumar, "Moisture sorption isotherms and evaluation of quality changes in extruded snacks during

storage," *Lebensmittel-Wissenschaft & Technologie*, vol. 74, pp. 448–455, 2016.

[49] P. P. Lewicki, "The applicability of the GAB model to food water sorption isotherms," *International Journal of Food Science and Technology*, vol. 32, no. 6, pp. 553–557, 1997.

[50] A. M. Goula, T. D. Karapantsios, D. S. Achilias, and K. G. Adamopoulos, "Water sorption isotherms and glass transition temperature of spray dried tomato pulp," *Journal of Food Engineering*, vol. 85, no. 1, pp. 73–83, 2008.

[51] T. Aksil, M. Abbas, M. Trari, and S. Benamara, "Water adsorption on lyophilized Arbutus unedo L. fruit powder: determination of thermodynamic parameters," *Microchemical Journal*, vol. 145, pp. 35–41, 2019.

[52] W. A. M. McMinn and T. R. A. Magee, "Thermodynamic properties of moisture sorption of potato," *Journal of Food Engineering*, vol. 60, no. 2, pp. 157–165, 2003.

[53] A. H. Al-Muhtaseb, W. A. M. McMinn, and T. R. A. Magee, "Water sorption isotherms of starch powders. Part 2: thermodynamic characteristics," *Journal of Food Engineering*, vol. 62, no. 2, pp. 135–142, 2004.

[54] P. C. Corrêa, A. L. D. Goneli, P. C. A. Júnior, G. H. H. de Oliveira, and D. S. M. Valente, "Moisture sorption isotherms and isosteric heat of sorption of coffee in different processing levels," *International Journal of Food Science and Technology*, vol. 45, pp. 2016–2022, 2010.

[55] D. Popovski and V. Mitrevski, "Some new four parameter models for moisture sorption isotherms," *Electronic Journal of Environmental, Agricultural and Food Chemistry*, vol. 3, no. 3, pp. 698–701, 2004.

[56] M. Peleg, "Assessment of a semi-empirical four parameter general model for sigmoid moisture sorption isotherms," *Journal of Food Process Engineering*, vol. 16, no. 1, pp. 21–37, 1993.

[57] C. R. Oswin, "The kinetics of package life. III. The isotherm," *Journal of the Society of Chemical Industry*, vol. 65, no. 12, pp. 419–421, 1946.

[58] M. Caurie, "A new model equation for predicting safe storage moisture levels for optimum stability of dehydrated foods," *International Journal of Food Science and Technology*, vol. 5, pp. 301–307, 1970.

[59] I. Kühn, "A new theoretical analysis of adsorption phenomena. Introductory part: the characteristic expression of the main regular types of adsorption isotherms by a single simple equation," *Journal of Colloid Science*, vol. 19, pp. 685–698, 1964.